An Unbiased Screen Identifies the DEP-1 Tumour Suppressor as a Phosphatase Controlling EGFR Endocytosis

Gabi Tarcic[1,6], **Shlomit K. Boguslavsky**[1,6,7], **Jean Wakim**[1], **Tai Kiuchi**[2,3], **Angela Liu**[4], **Felicia Reinitz**[4], **David Nathanson**[4], **Takamune Takahashi**[5], **Paul S. Mischel**[4], **Tony Ng**[2], and **Yosef Yarden**[1,*]

[1] Department of Biological Regulation, The Weizmann Institute of Science, Rehovot, Israel

[2] Richard Dimbleby Department of Cancer Research, Randall Division & Division of Cancer Studies, King's College London

[3] Guy's Medical School Campus, Breakthrough Breast Cancer Research Unit, Guy's Hospital, King's Health Partners AHSC, London, UK

[4] Department of Pathology and Laboratory Medicine, David Geffen School of Medicine, University of California, Los Angeles, Los Angeles, CA 90095, U.S.A

[5] Vanderbilt University Medical Center, Vanderbilt TN, U.S.A

Abstract

Background—The epidermal growth factor (EGF) stimulates rapid tyrosine phosphorylation of EGF-receptor (EGFR). This event precedes signalling from both the plasma membrane and from endosomes, and it is essential for recruitment of an ubiquitin ligase, CBL, that sorts activated receptors to endosomes and degradation. Because hyper-phosphorylation of EGFR is involved in oncogenic pathways, we performed an unbiased screen of siRNA oilgonucleotides targeting all human tyrosine phosphatases.

Results—We report the identification of PTPRK and PTPRJ (DEP-1) as EGFR-targeting phosphatases. DEP-1 is a tumour suppressor that dephosphorylates, thereby stabilizes EGFR by hampering its ability to associate with the CBL-GRB2 ubiquitin ligase complex. DEP-1 silencing enhanced tyrosine phosphorylation of endosomal EGFRs and, accordingly, increased cell proliferation. In line with functional interactions, EGFR and DEP-1 form physical associations, and EGFR phosphorylates a substrtae trapping mutant of DEP-1. Interestingly, the interactions of DEP-1 and EGFR are followed by physical segregation: whereas EGFR undergoes endocytosis, DEP-1 remains confined to the cell surface.

Conclusions—EGFR and DEP-1 physically interact at the cell surface and maitain bidirectional enzyme-substrate interactions, which are relevant to their respective oncogenic and tumor suppressive functions. These observations highlight the emerging roles of vesicular trafficking in malignant processes.

*Corresponding author: Department of Biological Regulation, Candiotty Building (room 302), The Weizmann Institute of Science, 1 Hertzl Street, Rehovot 76100, Israel. Tel. 972-8-9343974, FAX: 972-8-9342488, yosef.yarden@weizmann.ac.il).
[6]These authors contributed equally to this work
[7]Present address: Program in Cell Biology, Hospital for Sick Children, Toronto, Ontario M5G 1X8, Canada

Introduction

The balanced action of protein tyrosine kinases (PTKs) and protein tyrosine phosphatases (PTPs) is considered a major switch of many signal transduction pathways [1]. Interestingly, both families include transmembrane receptor-like enzymes, namely receptor tyrosine kinases (RTKs) and the less understood receptor-like PTPs (RPTPs). This divergence is exemplified by the epidermal growth factor receptor (EGFR) [2]. Upon EGF binding and subsequent structural alterations, receptor dimers are stabilized, thereby allowing activation of the intrinsic kinase domain and self-phosphorylation. Concomitant with transfer of active receptors from the plasma membranes to endosomes, phosphorylated tyrosine residues of EGFR act as docking sites for adaptors and enzymes that activate either stimulatory pathways, such as the mitogen-activated protein kinase (MAPK), or inhibitory cascades, like the CBL ubiquitin ligase. By ubiquitinylating EGFR, CBL instigates a process mediated by four endosomal sorting complexes (ESCRTs), culminating in lysosomal degradation of EGFR [3].

Several PTPs have been identified as candidate regulators of EGFR. For instance, EGFR phosphorylation was reduced upon inducible expression of RPTPsigma [4]. Other examples include PTPN1/PTP1B [5,6] and PTPN2/TCPTP [7]. Notably, PTP1B-mediated dephosphorylation of EGFR requires receptor endocytosis [8]. On the other hand, TCPTP is activated at the plasma membrane by a collagen–binding integrin, to negatively regulate EGFR [9]. Finally, forced co-expression of EGFR and various RPTPs enabled identification of RPTP-kappa as an enzyme capable of reducing EGFR phosphorylation [10].

The present study employed a siRNA library representing all human PTPs to identify PTPs able to catalytically interact with EGFR. The screen identified a candidate EGFR-targeting RPTP, namely DEP-1 (Density Enhanced Phosphatase-1, also designated CD148, PTP-eta and PTPRJ). Consistent with the induction of DEP-1 expression in contact-inhibited cells [11], the corresponding gene is often deleted or mutated in carcinomas [12], and DEP-1 exhibits tumour-suppressor activity when ectopically overexpressed [13–16]. Several previous studies identified RTK substrates of DEP-1, including the vascular endothelial growth factor (VEGF) receptor [17–19]. Beyond the unbiased identification of EGFR as a substrate for DEP-1, the results we present shed light on the molecular details of RTK-RPTP interactions: EGFR-DEP complexes exist at the cell surface prior to ligand binding. On binding of EGF, DEP-1 dephosphorylates, thereby stabilizes EGFR and inhibits signalling. Eventually, EGFR undertakes a route leading to endosomes and lysosomes, but DEP-1 remains at the cell surface. The implications of this segregation are discussed in the context of compartmentalized EGFR signalling and the diverse involvement of derailed endocytosis in cancer [20].

Results

An Unbiased Screen Identifies DEP-1 as a Suppressor of EGFR Signalling and Degradation

To substantiate the role for PTPs in EGF-induced phosphorylation events, we treated HeLa cells with two different phosphatase inhibitors, then stimulated with EGF (Fig. 1A). A mixture of H_2O_2 and sodium orthovanadate (HV), which potently but non-specifically inhibits PTPs [21], caused a significant increase in both basal and EGF-induced receptor phosphorylation (Fig. 1A). A vitamin K derivative, Compound 5, a mild inhibitor of PTPs [22], exerted similar,

but weaker effects (Fig. 1A), implying that PTPs critically regulate both basal and EGF-driven receptor phosphorylation.

To identify PTPs that underlay dephosphorylation of EGFR, we screened all human PTPs using a library of siRNA oligonucleotides collectively targeting 38 PTPs. Pools of four oligonucleotide were transfected into cells, and 48 hours later the cells were stimulated with EGF (see a flow diagram in Supplementary Fig. S1). Thereafter, whole cell lysates were immunoblotted with antibodies to EGFR, phosphotyrosine (pY99), and antibodies to the active form of ERK1/2. The library was independently screened twice, and candidates displaying undetectable mRNA levels in HeLa cells (Supplementary Table S1) were eliminated. The screens repeatedly identified PTPRK and DEP-1 (see examples in Figs. 1B and 1C). Notably, PTPRK has previously been identified on the basis of co-expressing PTPs together with EGFR in receptor-null cells [10], whereas the DEP-1 ortholog of *C. elegans* negatively regulates the worm's EGFR [23].

To validate the knockdown effect of the pool of four siRNA oligonucleotides, collectively targeting DEP-1, we tested individual components, each targeting a distinct part of the DEP-1 transcript. This experiment confirmed that all four independent siRNAs were able to reduce expression of DEP-1 (Supplementary Fig. S2). Next, we transfected HeLa cells with the pool of siRNA oligonucleotides and stimulated them with EGF (Fig. 1D). This experiment demonstrated effective siRNA-mediated inhibition of DEP-1 expression, and a concomitant enhancement of receptor phosphorylation (peaking at 15 min; Fig. 1E). In addition, DEP-1 knockdown accelerated EGFR degradation, and this effect was evident as early as 5 minutes after EGF stimulation (Fig. 1D). By employing commercially available antibodies, which are supposed to recognize specific tyrosine phosphorylation sites of EGFR, we found that depletion of endogenous DEP-1 non-selectively increased receptor phosphorylation, affecting all three sites we analyzed (tyrosines 1045, 1068 and 1173; data not shown). Last, consistent with enhanced phosphorylation and accelerated degradation of EGFR, we observed in DEP-1-depleted HeLa cells an increase in EGF-stimulated ERK1/2 activation, and an earlier decay relative to control cells (Fig. 1D).

Knockdown of DEP-1 Enhances Receptor Phosphorylation in Endosomes

To extend the functional analyses of EGFR-DEP-1 interactions to a cellular outcome, we referred to glioblastoma multiforme (GBM), an aggressive brain tumor often presenting over-active EGFRs. As a first step, we screened several GBM cell lines and identified Ln229 cells as high expressors of DEP-1 (Fig. 2A). Next, we used siRNA-DEP-1 to achieve effective knockdown. Most important, we found that knockdown of DEP-1 resulted in remarkable enhancement of EGFR phosphorylation (Fig. 2B), and this associated with increased cell proliferation (Fig. 2C; p=0.001). These results confirmed that mammalian DEP-1, similar to the invertebrate version, negatively regulates EGFR signaling, which prompted us to analyze the underlying mechanisms.

Our next set of experiments employed siRNA-treated HeLa cells, immunofluorescence and antibodies specific to EGFR or to phosphorylated tyrosine 1173 (pY1173). As expected, following stimulation with EGF (10 min), the receptor redistributed to endosomes (Fig. 2D). Image analyses revealed that the intensity of endosomal pY1173 was elevated in the majority (67%) of siDEP-1-treated cells, as compared to siControl cells (16%; Figs. 2D and 2E). Hence, we compared the vesicular pY1173 signal (n~50; >25 cells) in control and DEP-1-depleted cells (Fig. 2E). This analysis confirmed that the fraction of pY1173-enriched endosomes was significantly higher in DEP-1-knockdown cells, as compared to control cells (p<0.001; *t* test).

In conclusion, depletion of endogenous DEP-1 indicated that the phosphatase normally restricts tyrosine phosphorylation of EGFR, thereby it curtails signaling, as well as cellular

proliferation, and prevents transfer of active receptors to endosomes. This latter observation is consistent with a previously inferred receptor inactivation phase, affiliated with transfer from the plasma membrane to endosomes [24].

DEP-1 Gain-of-function Decreases Signalling Downstream to EGFR and Inhibits Ligand-induced Receptor Degradation

We next employed ectopic expression of DEP-1 to examine possible reciprocal effects to those reflected by siRNA-treated cells. Forty-eight hours following transfection with a plasmid encoding wild type (WT), HA-tagged DEP-1, HeLa cells were stimulated with EGF and whole cell extracts analyzed (Figs. 3A and 3B). DEP-1 overexpression reduced ligand-induced phosphorylation, as well as retarded receptor degradation. For example, by 60 minutes of stimulation, only a small fraction of EGFR escaped degradation; ectopic DEP-1 not only increased this fraction, but almost completely erased its tyrosine phopshorylation (Fig. 3B). Additionally, the decrease in EGFR activation was followed by decreased activation of ERK1/2 (Fig. 3A and 3C). Moreover, the effect of DEP-1 on MAPK activation was reflected in reduced transcription of the *FOS* gene (Fig. 3C).

To corroborate a model of DEP-1-enabling escape from degradation, we applied immunofluorescence and WT or a catalytically inactive mutant of DEP-1-HA (C1239S; denoted CS). Cells were either un-stimulated or stimulated with EGF for 10 min, then stained using an antibody to HA or to phosphorylated tyrosine 1173 of EGFR (pY1173; Fig. 3D). Ectopic WT-DEP-1 localized to the plasma membrane, as well as to polar peri-nuclear sites, which may correspond to biosynthetic compartments. Unlike un-stimulated cells, which displayed very weak pY1173 fluorescent signal (Fig. 3D; panels b and e), EGF stimulation remarkably increased pY1173 (compare panels b and i). Moreover, whereas the pY1173 signal of untrasfected cells largely corresponded to endosomes containing the endogenous EGFR of HeLa cells, 95% of WT-DEP-1 expressing cells displayed no (or very weak) punctate pY1173 staining (Figs. 3D and 3E). In sharp contrast to WT-DEP-1, vesicular pY1173-EGFR was detectable in most cells expressing the mutant form of the phosphatase (Fig. 3D, l-n, and Fig. 3E). Only in a small fraction of CS-DEP-1-expressing cells did we observe a reduction in vesicular pY1173 (Fig. 3E), suggesting that DEP-1 strongly inhibits removal of active EGFR molecules from the cell surface into endosomes. In conclusion, the results shown in Figure 3 indicate that DEP-1 can dephosphorylate EGFR at the cell surface; this phosphatase activity is responsible for blocking endocytosis of active receptors and for stabilizing a de-phosphorylated form of EGFR at the plasma membrane.

EGFR and DEP-1 Co-localize and Maintain Bi-directional Interactions

The ability of DEP-1 to dephosphorylate EGFR molecules predicted physical interactions that are confined to the cell surface. To test this model, we constructed a mutant of DEP-1, whose conserved aspartate 1205 has been replaced by an alanine (DA mutant), an approach developed for PTP1B [5]. Mutagenesis of the invariant catalytic aspartate converts an active enzyme into a "substrate trap". This mutant did not alter localization of EGFR (Fig. 4A), and like WT-DEP-1 and CS, displayed extensive co-localization with EGFR (Fig. 4A). Notably, both proteins localized almost exclusively to the cell surface, and their co-localization was most prominent at cell borders (arrows in Fig. 4A).

We next employed a co-immunoprecipitation approach to examine possible physical interactions between EGFR and DEP-1. However, immunoprecipitates of both EGFR and DEP-1 (WT and DA) contained undetectable traces of the other molecule (data not shown), suggesting that due to rapid turnover of many substrate molecules (i.e., EGFRs) by a single enzyme molecule (i.e., DEP-1), their physical interactions are very weak and transient. Hence, we adopted an *in vitro* assay that employed detergent-solubilized EGFR (from A431 cells) and

a bacterially expressed intracellular domain of DEP-1 fused to glutathione S-transferase (GST-DEP-1). Prior to lysis, intact A431 cells were incubated with a radio-labeled EGF, then subjected to covalent crosslinking that enables tgging EGFR with the radioactive ligand [25]. Unlike the WT form of GST-DEP-1, the DA mutant robustly interacted with EGFR (Fig. 4B). Two control experiments indicated specific interactions: first, both GST alone and CS displayed no pull-down activity. Second, pretreatment of cells with vanadate, a PTP inhibitor that binds to the catalytic site, reproducibly decreased the signal.

We next asked whether EGFR could trans-phosphorylate DEP-1 within the constitutive complex. Unlike CS and WT-DEP-1, which displayed no tyrosine phosphorylation upon ectopic expression in HeLa cells, the DA mutant presented weak phosphorylation on tyrosine residues prior to stimulation with EGF (Fig. 4C). This signal was reproducibly enhanced following a short (10 minute) stimulation with EGF. In line with direct involvement of EGFR's kinase activity, a specific inhibitor, AG1478, effectively reduced tyrosine phosphorylation of the DA mutant.

Biophysical Measurements of the Non-covalent Interactions Between EGFR and DEP-1

To further characterize the nature of the interactions between EGFR and DEP-1, we assayed the efficiency of Forster resonance energy transfer (FRET) between fluorescent derivatives, namely: EGFR-mRFP and DEP-1-WT-EGFP (or the respective DA and CS mutants), using fluorescence lifetime imaging microscopy (FLIM), as described [26–28]. Because of suboptimal expression of DEP-1-EGFP and EGFR-mRFP, relatively low FRET efficiencies (4%) were observed in co-transfected HeLa cells. Hence, we used MCF7 mammary cancer cells (Fig. 5). The fluorescence lifetime of DEP-1-WT-EGFP, the DA and CS mutants were remarkably reduced by co-expression of EGFR-mRFP, which indicate FRET occurs between DEP-1-EGFP and EGFR-mRFP (Figs. 5A–5C). However no significant change in FRET signal was detectable upon EGF stimulation in both the WT protein and the CS mutant. Still, DA demonstrated a significant increase in FRET signal upon EGF stimulation (Figs. 5B and 5D). These data are consistent with the ability of the DA mutant to bind activated EGFR (Fig. 4B), as well as undergo phosphorylation on stimulation with EGF (Fig. 4C). In conclusion, the biophysical measurements suggest that DEP-1 and EGFR preexist in a physical complex prior to ligand stimulation. On stimulation, the receptors are better bound by DEP-1 in a rapid and reversible manner, as this increase can only be seen in the presence of a substrate trap (DA) form of DEP-1.

DEP-1 Inhibits EGFR Internalization and Remains at the Cell Surface After EGFR is Internalized

Because DEP-1-overexpresing cells displayed virtually no tyrosine phosphorylated EGFRs in endosomes (Fig. 3D), we addressed the possibility that the phosphatase inhibits internalization of active EGFRs. Employing flow cytometry we found that following 10 minutes of stimulation with EGF, 71.9% of surface EGFR molecules translocated from the surface of siDEP-1-treated cells, as compared to only 47.7% in siControl cells (Fig. 6A). Conversely, 52.6% of surface receptors internalized in cells transfected with a control vector, whereas only 30.2% of the receptors underwent internalization in DEP-1-overexpressing cells (Fig. 6B). It is notable that only a fraction of HeLa cells undergo transfection. Hence, signal magnitude and the consistency of these two sets of results clearly indicate that DEP-1 decelerates the rate of ligand-induced EGFR internalization.

Next, we asked whether DEP-1 escorts EGFR to endosomal compartments. To address this question, HeLa cells were stimulated with a fluorescently labeled EGF (Fig. 6C). Whereas fluorescently labeled EGF efficiently translocated into endosomes, DEP-1 molecules remained at the cell surface (Fig. 6C), implying molecular segregation. To further address this scenario,

HeLa cells were stimulated with EGF, surface-labeled with antibodies to EGFR or to DEP-1, and both surface proteins quantified by flow cytometry (Fig. 6D). As expected, this analysis revealed that 60% of surface-localized EGFR molecules efficiently internalized after 15 minutes, but essentially all DEP-1 molecules remained at the cell surface. As a final test we asked whether a fraction of DEP-1 reaches the early endosomal compartment characterized by the presence of the small GTP-binding protein RAB5. As expected, a RAB5-GFP fusion protein localized to intracellular vesicles, but the co-expressed HA-DEP-1 showed little, if any, co-localization (Supplementary Figure S3). In conclusion, dephosphorylation by DEP-1 effectively decelerates the rate of EGFR internalization. Eventually, EGFR molecules are internalized, whereas DEP-1 molecules remain at the cell surface, perhaps in order to process other types of RTKs, as well as newly delivered EGFR molecules.

DEP-1 Disrupts Physical Association of an Ubiquitin Ligase Complex with EGFR Molecules and Impairs Its Activation

The distinct fates of EGFR and DEP-1 raised the possibility that protein ubiquitinylation, which underlies endocytic sorting, would differentiate between the two fates. To test this scenario, HeLa cells ectopically expressing WT-DEP-1 were stimulated with EGF and the ubiquitinylation status of both EGFR and DEP-1 was tested. The results confirmed rapid, EGF-induced ubiquitinylation of EGFR (Fig. 6E). DEP-1, on the other hand, displayed relatively weak ubiquitinylation, which was not affected by EGF, in line with different molecular fates. To test the hypothesis that DEP-1 disrupts receptor ubiquitinylation, we expressed it in HeLa cells, briefly stimulated with EGF and assessed EGFR ubiquitinylation. While the WT form of DEP-1 caused a decrease in EGF-induced receptor ubiquitinylation, the CS mutant exerted no marked effect (Fig. 6F). This observation corroborated the assumption that DEP-1 modulates EGFR trafficking, and also raised the possibility that DEP-1 regulates interactions of the underlying ubiquitin ligase, c-CBL, with EGFR [29]. To test this we examined the interaction of EGFR with c-CBL, as well as with the CBL's adaptor protein, GRB2 [30]. As predicted, ectopic expression of DEP-1 diminished interactions of EGFR with both c-CBL and GRB2 (Fig. 7A). Because c-CBL's activation is achieved via tyrosine phosphorylation we tested the effect of DEP-1 on modification of a major site of phosphorylation, namely tyrosine 731. Upon DEP-1 overexpression, c-CBL displayed reduced phosphorylation on this site compared to control cells (Fig. 7B). This result offers a mechanism by which DEP-1 affects EGFR trafficking: by dephosphorylating EGFR, and possibly also SRC family kinases involved in phosphorylation of c-CBL [31,32], DEP-1 reduces activation of c-CBL and its recruitment to the activated EGFR, hence inhibiting subsequent receptor internalization and degradation.

In summary, by dephosphorylating EGFR at the cell surface, DEP-1 reduces activation and subsequent recruitment of a dedicated ubiquitin ligase complex (i.e., CBL-GRB2), and inhibits both receptor ubiquitinylation and downstream signalling. Consequently, surface-localized receptors undergo inactivation, their translocation to endosomes is delayed, and those receptors that eventually reach the endocytic compartment are largely disarmed (see model in Fig. 7C).

Discussion

By employing an unbiased screen of all human PTPs, we identified DEP-1/PTPRJ as a phosphatases acting on EGFR. Because EGFR drives several types of malignancies in human [reviewed in [2]], and DEP-1 acts as a suppressor of several human tumours, including colon, lung, breast [12], and thyroid cancer [33], these observations shed new light on the molecular mechanisms enabling DEP-1 to exert tumour-suppressive activities. Similarly important is the finding that DEP-1 inhibits both receptor activation at the plasma membrane and transfer of active receptors to endosomes, while it remains confined to the cell surface (see model in Fig.

7C). These findings explain the previously observed inactivation-reactivation sequel of EGFR while en route to endosomes [24], and they also illuminate from a new perspective existing models attributing signalling capabilities to endosomal EGFRs [34].

RTKs Provide a Potential Mechanistic Basis for Tumour Suppression by DEP-1

Our screening strategy represents the first exhaustive search for PTPs specific to EGFR. In support of the reliability of our strategy, the two enzymes we identified, namely RPTP-kappa and DEP-1, have respectively been reported as a regulator of EGFR in mammalian cells [10], and an enzyme whose invertebrate ortholog genetically interacts with EGFR of *C. elegans* [23]. Several other screening strategies have previously been employed, including the utilization of substrate trapping mutants, which identified PTP-1B [6] and TC-PTP [7] as EGFR regulators. The latter enzyme mediates suppression of EGFR by integrins [9], suggesting that screening assays performed on distinct extracellular matrices may identify different enzymes.

Here we demonstrate that DEP-1 suppresses growth signals initiated by EGFR (Fig. 2C). Likewise, previous reports documented an ability of DEP-1 to suppress signals emanating from other RTKs, such as PDGF-beta receptors [35], VEGF-receptors [17] and c-Met/HGF-receptor [19]. Taken together with our results, these observations suggest that DEP-1 acts as a pan-RTK suppressor of growth factor signals. In combination with pan-RTK functions, our results attribute suppression of tumorigenesis to the ability of DEP-1 to dephosphorylate EGFR and concurrently inhibit receptor translocation to endosomes and to the nucleus, compartments believed to support long-term RTK signalling [36]. Supporting lines of evidence include the ability of an overexpressed DEP-1 to induce differentiation and suppress tumour cell growth [14,15]. In the same vein, a transforming acute retrovirus reduces DEP-1 expression [37] and, conversely, forced expression of DEP-1 suppresses transformation by viral oncogenes [15]. Finally, the gene encoding DEP-1 has been identified as a candidate for a murine colon cancer susceptibility locus [*SCC1*; [12]]. Loss of heterozygosity (LOH) of the human gene is frequently found in colon, breast [38] and thyroid [39] cancer.

While no previous study associated DEP-1 with a defect in the transfer of active receptors to endosomes, several published reports, such as DEP-1-mediated reduction in MAPK signalling [40], as well as stabilization of the cell cycle inhibitor p21-KIP1 [15], are consistent with a mechanism involving inhibition of signals emanating from both the plasma membrane and from intracellular compartments. When combined with the reported ability of DEP-1 to mediate contact inhibition of cell growth [11], our results suggest the following explanation for the tumour suppressive activity of DEP-1: by dephosphorylating EGFR at the plasma membrane and by halting transfer of active receptors to intracellular sites of signal generation, DEP-1 confers contact inhibition of cell growth. Once this activity of DEP-1 is compromised by LOH or by other mechanisms, epithelial cells are free to fully respond to EGF and to other growth factors (e.g., HGF and VEGF), thus promoting cell proliferation, migration and recruitment of blood vessels essential for tumour progression.

Functional Implications of the Ability of DEP-1 to Inhibit Endocytosis of EGFR

By injecting EGF into the portal vein of rats and analyzing hepatic plasma membrane and endosomal fractions, Bergeron and colleagues inferred a pre-endocytosis desensitization step [24]. They later found that the endosomal, tyrosine-phosphorylated receptors nucleate a signalling complex containing SHC and the RAS guanine nucleotide exchange factor, mSOS [41]. Similarly, other researchers identified a pool of active, ligand-bound PDGF-beta receptors in endosomes [42]. These studies, along with a large series of analyses addressing the nerve growth factor receptor, lead to the realization that the RTK-harboring endosome serves as a platform of signal transduction events [34]. In view of the strict compartmentalization of DEP-1 to the plasma membrane and the segregation from internalizing receptors, the concept of

'signalling endosomes' may be revised as follows: while at the plasma membrane, activation of RTKs like EGFR is tightly controlled by DEP-1. However, upon translocation to endosomes and segregation from DEP-1, receptor auto-phosphorylation is relieved, which licenses endosomal signalling.

In summary, our study identified a novel RTK regulatory pathway: by dephosphorylating EGFR at the plasma membrane and limiting endocytosis of active receptors, DEP-1 tightly controls EGFR's ability to generate intracellular signals. This regulatory pathway plays an important role during embryonic development of invertebrates [23], and it is manipulated in human carcinomas, whose DEP-1 frequently undergoes genetic alterations [12,38]. Future studies will address the relevance of the DEP-1 regulatory module to other pairs of RTKs and the respective receptor-like PTPs.

Experimental Procedures

Reagents and Antibodies

Monoclonal antibodies to EGFR were from Upstate, Alexis Biotechnology, or they were generated in our laboratory. Antibodies to specific phosphotyrosines of EGFR were from Cell Signaling or Zymed. Other antibodies were from R&D (DEP-1), Babco (ubiquitin), Roche (hemagglutinin), Jackson ImmunoResearch Laboratories (Cy2-conjugated), or Santa-Cruz Biotechnology. EGF conjugated to Alexa Fluor 488 streptavidin was from Molecular Probes.

Cellular Treatments and Transfection

Transient plasmid expression was achieved using the jetPEI transfection reagent (Polyplus-Transfection). siRNA transfection was carried out using the HiperFect transfection reagent (Qiagen). Delivery effectiveness of siRNA was determined using the KDalert assay kit (Ambion).

Expression Vectors and siRNA Oligonucleotides

Plasmids (pSRα) encoding HA (hemagglutinin epitope)-tagged DEP-1 [wild type (WT), C1239S (CS) and D1205A (DA)] have been described [43]. EGFP tagged DEP-1 was a kind gift from Dr. Arne Östman. siDEP-1 and control siRNA oligonucleotides were obtained from Dharmacon (DEP-1; accession number M-008476-01, siControl; accession number D-001206-14; Supplementary Table S2). RAB5-GFP was a kind gift of Dr. Sima Lev.

Real Time Quantitative PCR

cDNA was generated using SuperScript first-strand synthesis kit (Invitrogen). Real-time PCR analysis was performed using DyNAmo HS SYBR Green qPCR kit (Finnzymes). All experiments were carried out in triplicates and normalized to beta-2 microglobulin RNA levels.

Immunoblotting, Immunoprecipitation and Pull-down Analyses

The procedures and content of buffers were essentially as described [29]. For pull-down, radio-labeled EGF (20ng/ml) was incubated for 2h at 4 °C with confluent A431 cells (10^7 cells). Following extensive washing, saline containing bis(succinimidyl) suberate (BS^3; 1mM) was incubated with the cells for 20 min at room temperature. The reagent was quenched in quenching solution (10mM Tris-HCl, pH 7.5, 200mM glycine and 2mM EDTA). Cells were harvested in saline, and solubilized in the absence or presence of 0.2mM sodium orthovavadate. Subsequently, glutathione beads bound to different GST proteins (0.05mg, each) were added, and the mixtures rotated for 12h at 4 °C, prior to washing and gel electrophoresis.

Immunofluorescence

Cells were treated as described [44]. Images of fixed cells were recorded using the DeltaVision System (Applied Precision) that included an Olympus IX71 inverted fluorescence microscope equipped with a charge-coupled camera (Photometrics), a 100W mercury lamp and excitation and emission filter wheels. Images were acquired with an Olympus plan ApoN 60x 1.42 N/A objective. pY1173 fluorescence intensity of EGFR-positive vesicles was determined by calculating the mean gray value within the selected vesicular areas. Fluorescence intensity was measured using VICTOR2 MultiLabel Counter (Perkin Elmer).

Cell Proliferation Assay

Cells grown in DME medium supplemented with 10% fetal bovine serum were transfected with siRNA nucleotides (25 nM) obtained from Applied Biosystems (DEP-1; cat # S230208 and scrambled; cat #AM4611). After 48 hours cells were re-plated in 96-well plates and following an overnight incubation, media were changed to 1% serum and relative cell proliferation was measured on day 0 and day 3 using the WST-1 Kit from Chemicon.

Flow Cytometry

The assay was carried out as described [45].

FRET Determination by Multiphoton Fluorescence Lifetime Imaging Microscopy Measurements

Fluorescence lifetime imaging (FLIM) was performed using a custom-built multi-photon system constructed around an upright 90i fluorescence microscope (Nikon) and similar to that described elsewhere [46].

Supplementary Material

Refer to Web version on PubMed Central for supplementary material.

Acknowledgments

References

1. Tonks NK. Protein tyrosine phosphatases: from genes, to function, to disease. Nat Rev Mol Cell Biol 2006;7:833–846. [PubMed: 17057753]

2. Citri A, Yarden Y. EGF-ERBB signalling: towards the systems level. Nat Rev Mol Cell Biol 2006;7:505–516. [PubMed: 16829981]

3. Katzmann DJ, Odorizzi G, Emr SD. Receptor downregulation and multivesicular-body sorting. Nat Rev Mol Cell Biol 2002;3:893–905. [PubMed: 12461556]

4. Suarez Pestana E, Tenev T, Gross S, Stoyanov B, Ogata M, Bohmer FD. The transmembrane protein tyrosine phosphatase RPTPsigma modulates signaling of the epidermal growth factor receptor in A431 cells. Oncogene 1999;18:4069–4079. [PubMed: 10435588]

5. Flint AJ, Tiganis T, Barford D, Tonks NK. Development of "substrate-trapping" mutants to identify physiological substrates of protein tyrosine phosphatases. Proc Natl Acad Sci U S A 1997;94:1680–1685. [PubMed: 9050838]

6. Liu F, Chernoff J. Protein tyrosine phosphatase 1B interacts with and is tyrosine phosphorylated by the epidermal growth factor receptor. Biochem J 1997;327(Pt 1):139–145. [PubMed: 9355745]

7. Tiganis T, Bennett AM, Ravichandran KS, Tonks NK. Epidermal growth factor receptor and the adaptor protein p52Shc are specific substrates of T-cell protein tyrosine phosphatase. Mol Cell Biol 1998;18:1622–1634. [PubMed: 9488479]

8. Reynolds AR, Tischer C, Verveer PJ, Rocks O, Bastiaens PI. EGFR activation coupled to inhibition of tyrosine phosphatases causes lateral signal propagation. Nat Cell Biol 2003;5:447–453. [PubMed: 12717446]

9. Mattila E, Pellinen T, Nevo J, Vuoriluoto K, Arjonen A, Ivaska J. Negative regulation of EGFR signalling through integrin-alpha1beta1-mediated activation of protein tyrosine phosphatase TCPTP. Nat Cell Biol 2005;7:78–85. [PubMed: 15592458]

10. Xu Y, Tan LJ, Grachtchouk V, Voorhees JJ, Fisher GJ. Receptor-type protein-tyrosine phosphatase-kappa regulates epidermal growth factor receptor function. J Biol Chem 2005;280:42694–42700. [PubMed: 16263724]

11. Ostman A, Yang Q, Tonks NK. Expression of DEP-1, a receptor-like protein-tyrosine-phosphatase, is enhanced with increasing cell density. Proc Natl Acad Sci U S A 1994;91:9680–9684. [PubMed: 7937872]

12. Ruivenkamp CA, van Wezel T, Zanon C, Stassen AP, Vlcek C, Csikos T, Klous AM, Tripodis N, Perrakis A, Boerrigter L, et al. Ptprj is a candidate for the mouse colon-cancer susceptibility locus Scc1 and is frequently deleted in human cancers. Nat Genet 2002;31:295–300. [PubMed: 12089527]

13. Iuliano R, Trapasso F, Le Pera I, Schepis F, Sama I, Clodomiro A, Dumon KR, Santoro M, Chiariotti L, Viglietto G, et al. An adenovirus carrying the rat protein tyrosine phosphatase eta suppresses the growth of human thyroid carcinoma cell lines in vitro and in vivo. Cancer Res 2003;63:882–886. [PubMed: 12591742]

14. Keane MM, Lowrey GA, Ettenberg SA, Dayton MA, Lipkowitz S. The protein tyrosine phosphatase DEP-1 is induced during differentiation and inhibits growth of breast cancer cells. Cancer Res 1996;56:4236–4243. [PubMed: 8797598]

15. Trapasso F, Iuliano R, Boccia A, Stella A, Visconti R, Bruni P, Baldassarre G, Santoro M, Viglietto G, Fusco A. Rat protein tyrosine phosphatase eta suppresses the neoplastic phenotype of retrovirally transformed thyroid cells through the stabilization of p27(Kip1). Mol Cell Biol 2000;20:9236–9246. [PubMed: 11094075]

16. Trapasso F, Yendamuri S, Dumon KR, Iuliano R, Cesari R, Feig B, Seto R, Infante L, Ishii H, Vecchione A, et al. Restoration of receptor-type protein tyrosine phosphatase eta function inhibits human pancreatic carcinoma cell growth in vitro and in vivo. Carcinogenesis 2004;25:2107–2114. [PubMed: 15231692]

17. Grazia Lampugnani M, Zanetti A, Corada M, Takahashi T, Balconi G, Breviario F, Orsenigo F, Cattelino A, Kemler R, Daniel TO, et al. Contact inhibition of VEGF-induced proliferation requires vascular endothelial cadherin, beta-catenin, and the phosphatase DEP-1/CD148. J Cell Biol 2003;161:793–804. [PubMed: 12771128]

18. Jandt E, Denner K, Kovalenko M, Ostman A, Bohmer FD. The protein-tyrosine phosphatase DEP-1 modulates growth factor-stimulated cell migration and cell-matrix adhesion. Oncogene 2003;22:4175–4185. [PubMed: 12833140]

19. Palka HL, Park M, Tonks NK. Hepatocyte growth factor receptor tyrosine kinase met is a substrate of the receptor protein-tyrosine phosphatase DEP-1. J Biol Chem 2003;278:5728–5735. [PubMed: 12475979]

20. Mosesson Y, Chetrit D, Schley L, Berghoff J, Ziv T, Carvalho S, Milanezi F, Admon A, Schmitt F, Ehrlich M, et al. Monoubiquitinylation regulates endosomal localization of Lst2, a negative regulator of EGF receptor signaling. Dev Cell 2009;16:687–698. [PubMed: 19460345]

21. Gordon JA. Use of vanadate as protein-phosphotyrosine phosphatase inhibitor. Methods Enzymol 1991;201:477–482. [PubMed: 1943774]

22. Onoda T, Iinuma H, Sasaki Y, Hamada M, Isshiki K, Naganawa H, Takeuchi T, Tatsuta K, Umezawa K. Isolation of a novel tyrosine kinase inhibitor, lavendustin A, from Streptomyces griseolavendus. J Nat Prod 1989;52:1252–1257. [PubMed: 2614420]

23. Berset TA, Hoier EF, Hajnal A. The C. elegans homolog of the mammalian tumor suppressor Dep-1/Scc1 inhibits EGFR signaling to regulate binary cell fate decisions. Genes Dev 2005;19:1328–1340. [PubMed: 15901674]

24. Lai WH, Cameron PH, Doherty JJ 2nd, Posner BI, Bergeron JJ. Ligand-mediated autophosphorylation activity of the epidermal growth factor receptor during internalization. J Cell Biol 1989;109:2751–2760. [PubMed: 2592404]

25. Goldman R, Levy RB, Peles E, Yarden Y. Heterodimerization of the erbB-1 and erbB-2 receptors in human breast carcinoma cells: a mechanism for receptor transregulation. Biochemistry 1990;29:11024–11028. [PubMed: 1980216]

26. Legg JW, Lewis CA, Parsons M, Ng T, Isacke CM. A novel PKC-regulated mechanism controls CD44 ezrin association and directional cell motility. Nat Cell Biol 2002;4:399–407. [PubMed: 12032545]

27. Ng T, Squire A, Hansra G, Bornancin F, Prevostel C, Hanby A, Harris W, Barnes D, Schmidt S, Mellor H, et al. Imaging protein kinase Calpha activation in cells. Science 1999;283:2085–2089. [PubMed: 10092232]

28. Barber PR, Ameer-Beg SM, Gilbey J, Carlin LM, Keppler M, Ng TC, Vojnovic B. Multiphoton time-domain fluorescence lifetime imaging microscopy: practical application to protein-protein interactions using global analysis. Journal of the Royal Society Interface 2009;6:S93–S105.

29. Levkowitz G, Waterman H, Ettenberg SA, Katz M, Tsygankov AY, Alroy I, Lavi S, Iwai K, Reiss Y, Ciechanover A, et al. Ubiquitin ligase activity and tyrosine phosphorylation underlie suppression of growth factor signaling by c-Cbl/Sli-1. Mol Cell 1999;4:1029–1040. [PubMed: 10635327]

30. Waterman H, Yarden Y. Molecular mechanisms underlying endocytosis and sorting of ErbB receptor tyrosine kinases. FEBS Lett 2001;490:142–152. [PubMed: 11223029]

31. Feshchenko EA, Langdon WY, Tsygankov AY. Fyn, Yes, and Syk phosphorylation sites in c-Cbl map to the same tyrosine residues that become phosphorylated in activated T cells. J Biol Chem 1998;273:8323–8331. [PubMed: 9525940]

32. Pera IL, Iuliano R, Florio T, Susini C, Trapasso F, Santoro M, Chiariotti L, Schettini G, Viglietto G, Fusco A. The rat tyrosine phosphatase eta increases cell adhesion by activating c-Src through dephosphorylation of its inhibitory phosphotyrosine residue. Oncogene 2005;24:3187–3195. [PubMed: 15735685]

33. Iervolino A, Iuliano R, Trapasso F, Viglietto G, Melillo RM, Carlomagno F, Santoro M, Fusco A. The receptor-type protein tyrosine phosphatase J antagonizes the biochemical and biological effects of RET-derived oncoproteins. Cancer Res 2006;66:6280–6287. [PubMed: 16778204]

34. Polo S, Di Fiore PP. Endocytosis conducts the cell signaling orchestra. Cell 2006;124:897–900. [PubMed: 16530038]

35. Kovalenko M, Denner K, Sandstrom J, Persson C, Gross S, Jandt E, Vilella R, Bohmer F, Ostman A. Site-selective dephosphorylation of the platelet-derived growth factor beta-receptor by the receptor-like protein-tyrosine phosphatase DEP-1. J Biol Chem 2000;275:16219–16226. [PubMed: 10821867]

36. Miaczynska M, Christoforidis S, Giner A, Shevchenko A, Uttenweiler-Joseph S, Habermann B, Wilm M, Parton RG, Zerial M. APPL proteins link Rab5 to nuclear signal transduction via an endosomal compartment. Cell 2004;116:445–456. [PubMed: 15016378]

37. Zhang L, Martelli ML, Battaglia C, Trapasso F, Tramontano D, Viglietto G, Porcellini A, Santoro M, Fusco A. Thyroid cell transformation inhibits the expression of a novel rat protein tyrosine phosphatase. Exp Cell Res 1997;235:62–70. [PubMed: 9281353]

38. Ruivenkamp C, Hermsen M, Postma C, Klous A, Baak J, Meijer G, Demant P. LOH of PTPRJ occurs early in colorectal cancer and is associated with chromosomal loss of 18q12–21. Oncogene 2003;22:3472–3474. [PubMed: 12776199]

39. Iuliano R, Le Pera I, Cristofaro C, Baudi F, Arturi F, Pallante P, Martelli ML, Trapasso F, Chiariotti L, Fusco A. The tyrosine phosphatase PTPRJ/DEP-1 genotype affects thyroid carcinogenesis. Oncogene 2004;23:8432–8438. [PubMed: 15378013]

40. Sacco F, Tinti M, Palma A, Ferrari E, Nardozza AP, Hooft van Huijsduijnen R, Takahashi T, Castagnoli L, Cesareni G. Tumor suppressor density-enhanced phosphatase-1 (DEP-1) inhibits the RAS pathway by direct dephosphorylation of ERK1/2 kinases. J Biol Chem. 2009

41. Di Guglielmo GM, Baass PC, Ou WJ, Posner BI, Bergeron JJ. Compartmentalization of SHC, GRB2 and mSOS, and hyperphosphorylation of Raf-1 by EGF but not insulin in liver parenchyma. EMBO J 1994;13:4269–4277. [PubMed: 7925272]

42. Sorkin A, Eriksson A, Heldin CH, Westermark B, Claesson-Welsh L. Pool of ligand-bound platelet-derived growth factor beta-receptors remain activated and tyrosine phosphorylated after internalization. J Cell Physiol 1993;156:373–382. [PubMed: 7688373]

43. Tsuboi N, Utsunomiya T, Roberts RL, Ito H, Takahashi K, Noda M, Takahashi T. The tyrosine phosphatase CD148 interacts with p85 regulatory subunit of PI 3-kinase. Biochem J. 2008

44. Katz M, Shtiegman K, Tal-Or P, Yakir L, Mosesson Y, Harari D, Machluf Y, Asao H, Jovin T, Sugamura K, et al. Ligand-independent degradation of epidermal growth factor receptor involves receptor ubiquitylation and Hgs, an adaptor whose ubiquitin-interacting motif targets ubiquitylation by Nedd4. Traffic 2002;3:740–751. [PubMed: 12230472]

45. Zwang Y, Yarden Y. p38 MAP kinase mediates stress-induced internalization of EGFR: implications for cancer chemotherapy. EMBO J 2006;25:4195–4206. [PubMed: 16932740]

46. Peter M, Ameer-Beg SM, Hughes MK, Keppler MD, Prag S, Marsh M, Vojnovic B, Ng T. Multiphoton-FLIM quantification of the EGFP-mRFP1 FRET pair for localization of membrane receptor-kinase interactions. Biophys J 2005;88:1224–1237. [PubMed: 15531633]
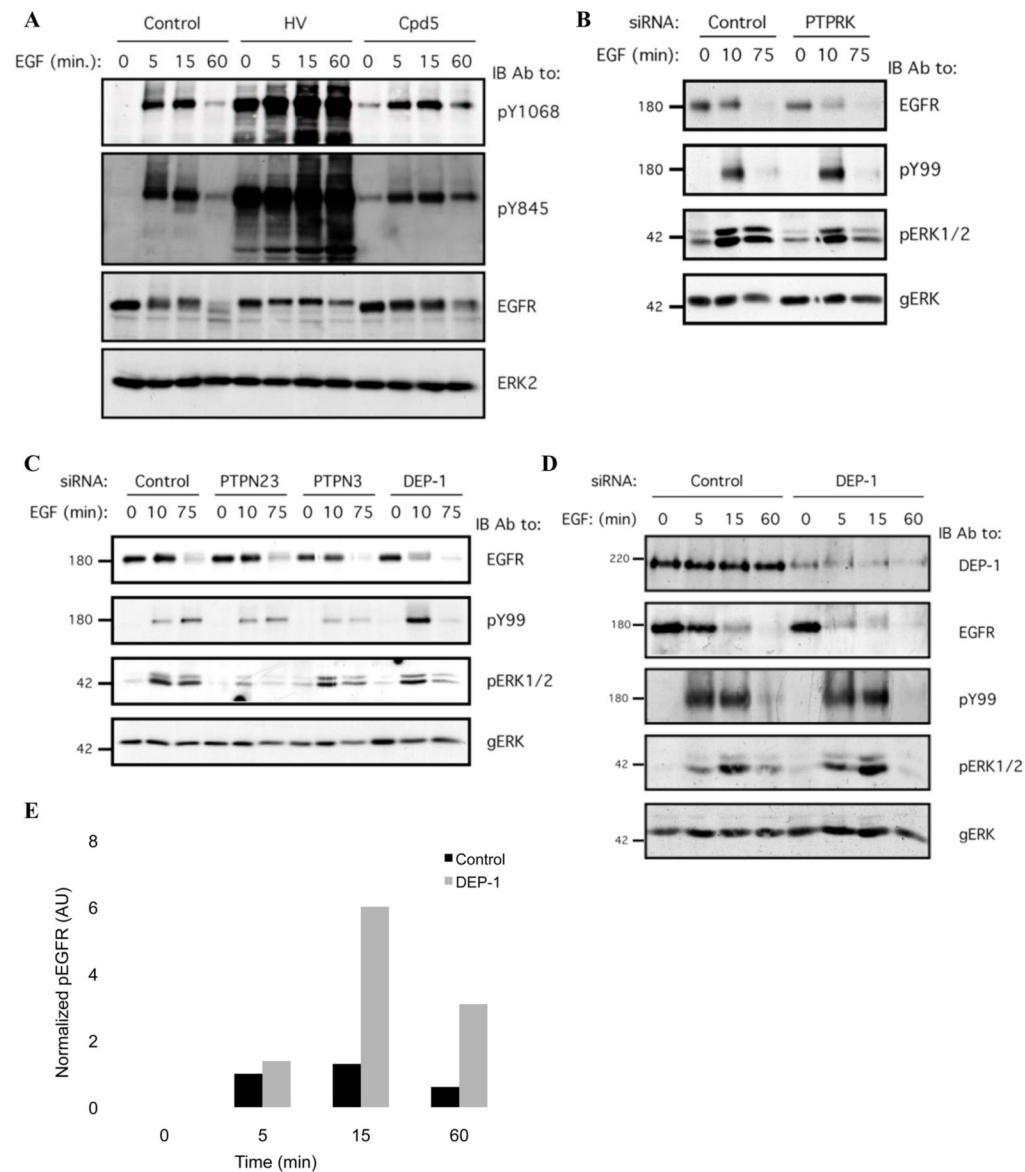
Figure 1. An Unbiased Genetic Screen Identifies PTPs Regulating EGF-mediated Receptor Phosphorylation and Degradation

(A) HeLa cells were serum-starved for 16h, then treated with either a mixture of H_2O_2 (0.2mM) and sodium orthovanadate (1mM; for 15min; HV), Compound 5 (Cpd5; 20mM; for 30 min) or with ethanol (control; 30 min), and then stimulated with EGF (20ng/ml) for the indicated time intervals. Whole cell lysates were blotted with the indicated antibodies.

(B and C) Mixtures of siRNA oligonucleotides were transfected into HeLa cells, which were then incubated for 32h and serum-starved for 16h. The cells were then stimulated with EGF (20ng/ml) for the indicated intervals and lysed. Whole cell lysates were blotted with the indicated antibodies, including an anti-phosphotyrosine antibody (pY99), and antibodies to the active (pERK) and general forms of ERK (gERK).

(D) HeLa cells were transiently transfected with DEP-1 siRNA oligonucleotides or with control siRNA (each at 10nM), incubated for 32h, serum-starved for 16h and stimulated with EGF (20ng/ml) for the indicated time intervals. Whole cell lysates were immunoblotted with the indicated antibodies.

(E) HeLa cells were treated and processed as in D. EGFR phosphorylation was quantified using densitometric analysis and normalized to total EGFR level. One representative experiments (n=3) is shown.
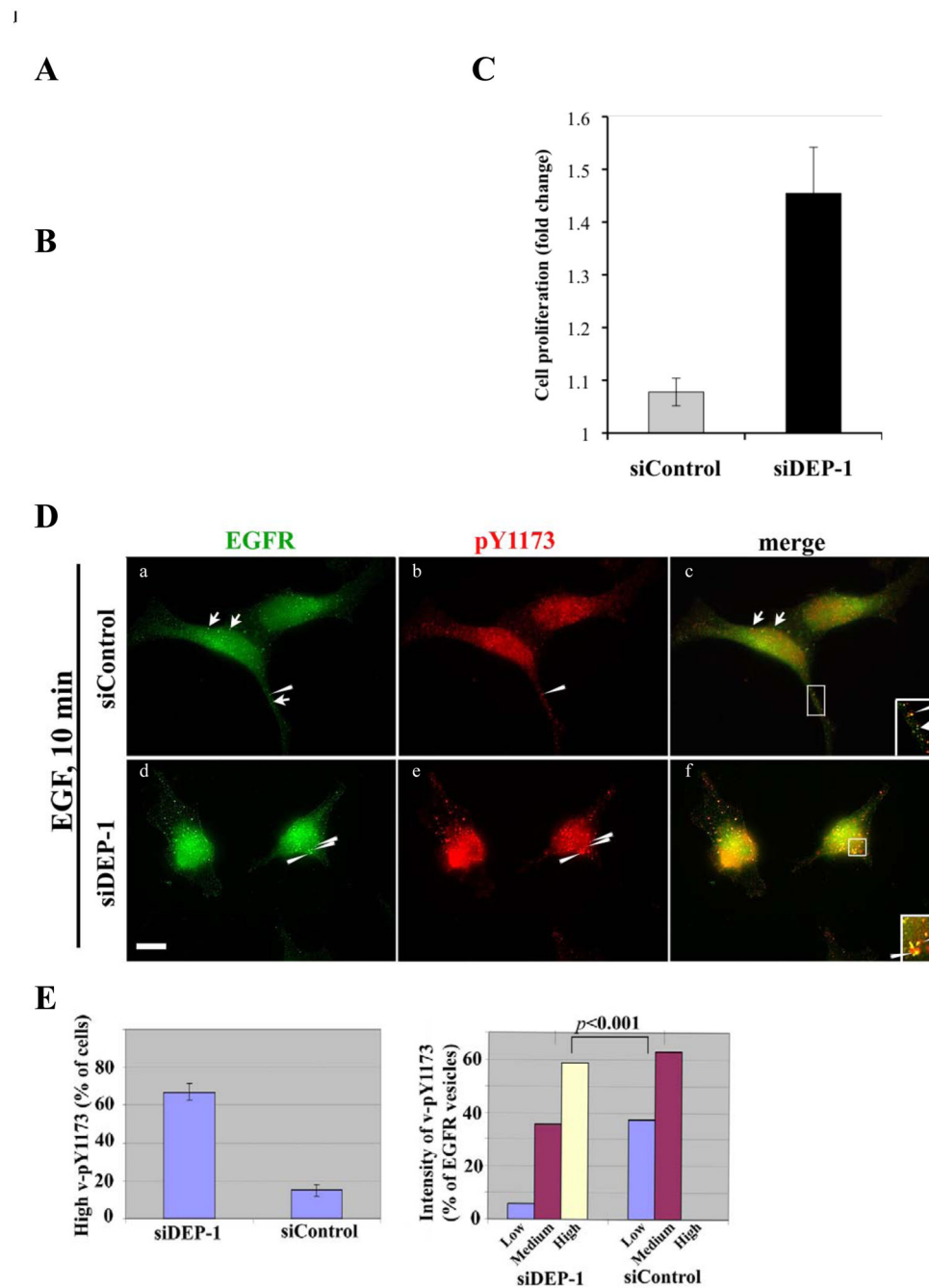
A

B

C

D

E

Figure 2. Knockdown of DEP-1 Increases Phosphorylation of Vesicular EGFRs and Enhances Proliferation of Glioblastoma Cells

(A) Whole extracts of Ln229 and T98 glioblastoma cells were immunoblotted with antibodies to DEP-1 or the p85 subunit of phosphoinositide 3-kinase.

(B) Ln229 cells were transfected with siRNA oligonucleotides targeting DEP-1 transcripts. Following 48h of incubation, cells were harvested for immunoblotting analysis.

(C) Ln229 cells were transfected with siRNA oligonucleotides targeting DEP-1 transcripts, then incubated for 48h and plated in 96-well plates under 1% serum. Proliferation was measured after 3 days and compared to day 1. An asterisk indicates $p= 0.001$.

(D) HeLa cells were transfected with DEP-1-siRNA (10nM; panels d, e, and f), or with control siRNA (panels a, b, and c), then stimulated with EGF (20ng/ml, 10 min). Thereafter, cells were analyzed by immunofluorescence using an antibody to EGFR or to phosphorylated EGFR (pY1173). Images were taken at the same exposure time. Arrowheads indicate vesicles positive for both EGFR and pY1173; arrows mark EGFR-positive, but pY1173 negative vesicles. Enlarged areas show internalized EGFR in vesicles. Scale bar: 10 μm.

(E) Left panel: The number of cells displaying >10 pY1173-positive vesicles are compared in DEP-1-siRNA- and control- treated HeLa cells. Data are expressed as mean±S.D. (bars) of three independent measurements. Right panel: Fluorescence intensities of pY1173-positive vesicles (n~50; 5 cells) were analyzed using NIH ImageJ software. The experiment was repeated twice.
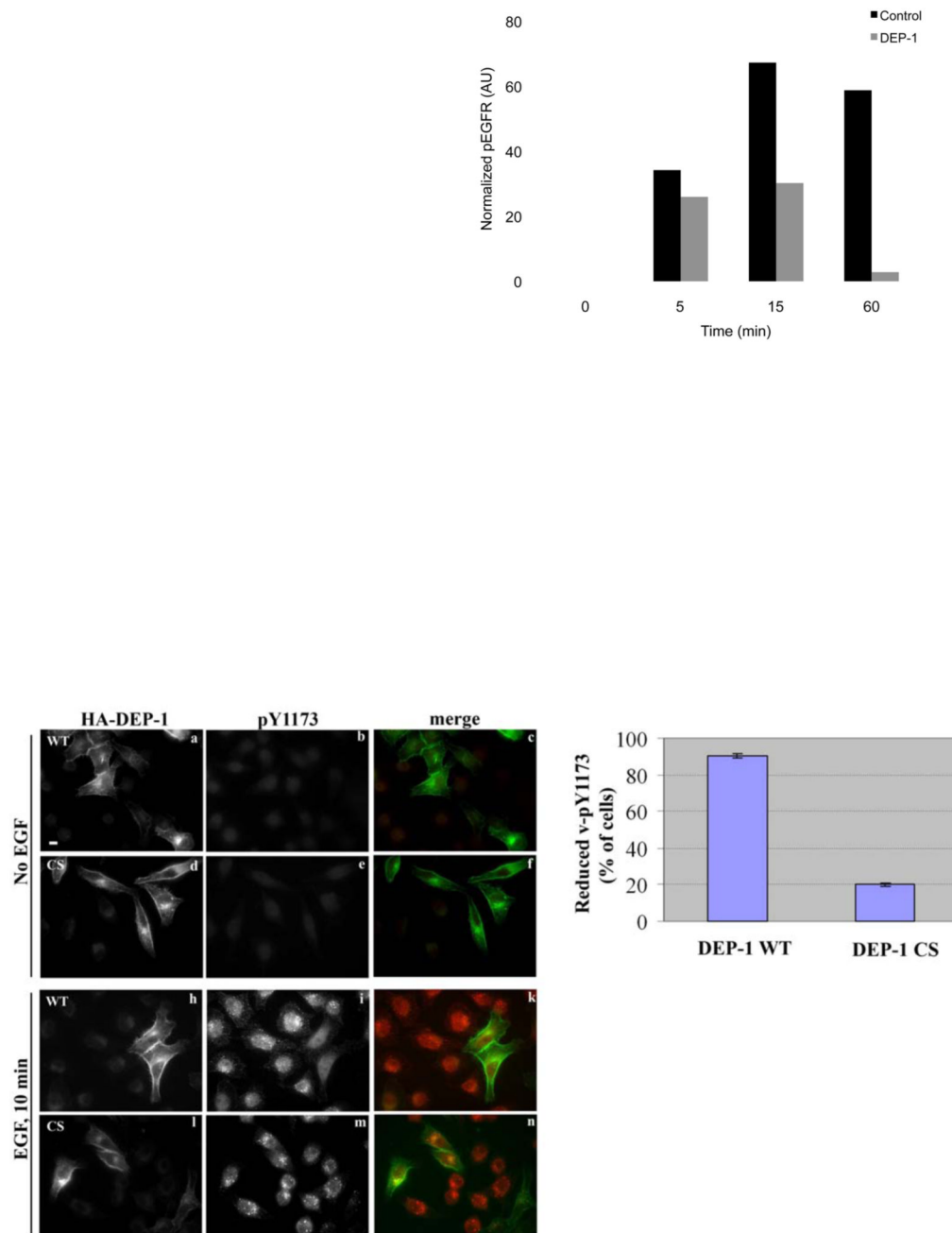
Figure 3. Ectopic DEP-1 Decreases Receptor Phosphorylation, Stabilizes EGFR and Inhibits Downstream Signalling

(A) HeLa cells were transfected with a plasmid encoding HA-tagged DEP-1, or with a control expression vector, then incubated for 32h, serum-starved for 16h, and stimulated with EGF (20ng/ml) for the indicated time intervals. Thereafter, cell extracts were analyzed by immunoblotting.

(B) HeLa cells were treated as in A. EGFR phosphorylation was quantified and normalized. One representative experiment (n=3) is shown.

(C) HeLa cells were treated as in A and stimulated with EGF (20ng/ml) for the indicated intervals. Left panel: cells were processed for immunoblotting and densitometry of pERK1/2

levels (normalized to total ERK2 level; gERK). Right panel: cells were lysed, total RNA was prepared and used for reverse transcription. Real-time PCR was carried out with *c-FOS* primers.

(D) HeLa cells were transfected with plasmids encoding wild type HA-DEP-1 (a-c, h-k), or a catalytically inactive mutant (CS; d-f, l-n), then incubated for 32h, serum-starved for 16h (a-f) and stimulated with EGF (20ng/ml) for 10min (h-n). Cells were then fixed and analyzed by immunofluorescence using an antibody to HA (a, d, h, l) or to phosphorylated EGFR (pY1173; b, e, i, m). Images of phosphorylated EGFR were taken at the same exposure time. Endogenous phosphorylated EGFR appears green and DEP-1 appears red. One representative experiment is shown (n=2). Scale bar: 10 μm.

(E) HeLa cells expressing DEP-1 (WT or CS) were treated as in D. The histogram compares the fractions of cells (±S.D.) displaying vesicular pY1173 in three independent measurements (>100 cells).
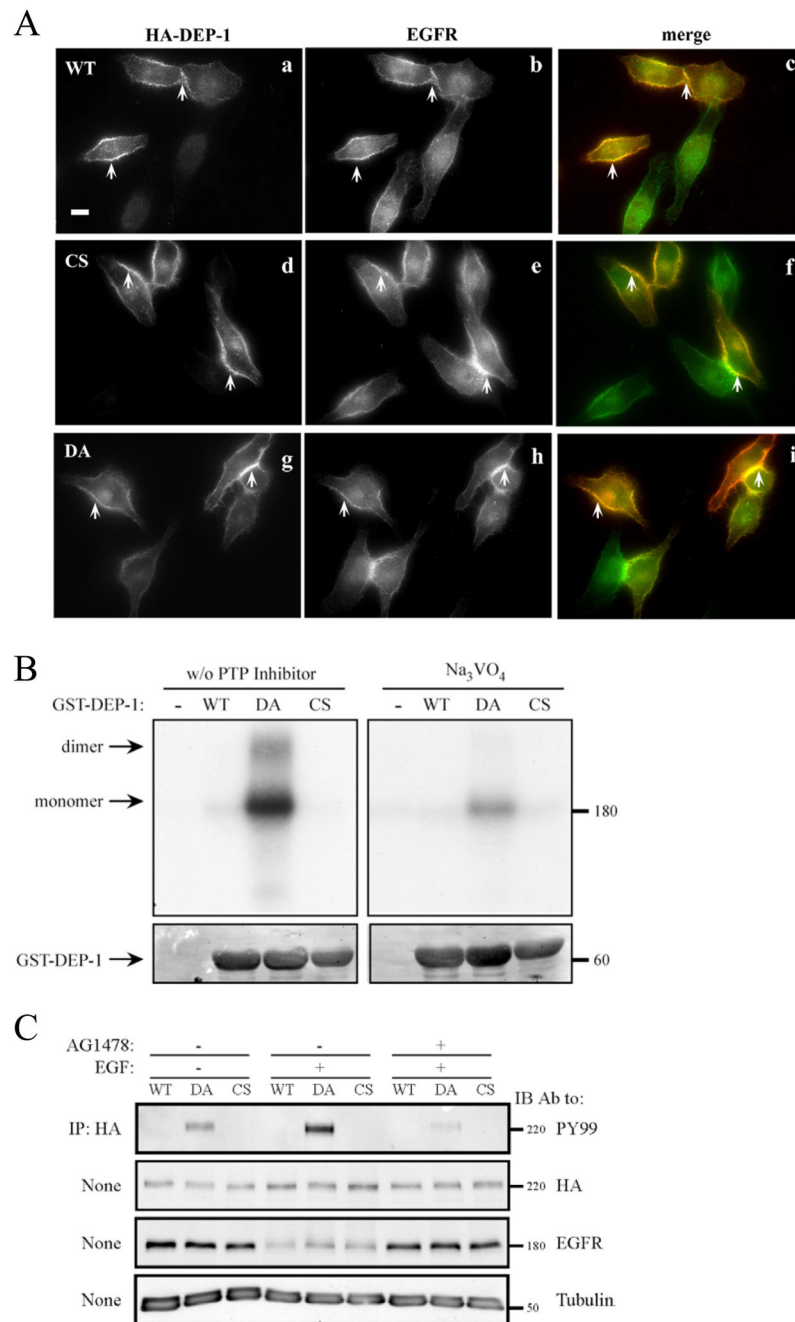
Figure 4. DEP-1 and EGFR Co-localize at the Cell Surface, Physically Interact and Maintain Bi-directional Enzymatic Interactions

(A) HeLa cells were transiently transfected with vectors encoding HA-tagged WT DEP-1 (a-c), a CS mutant (d-f), or with a DA mutant (g-i). Thereafter, cells were incubated for 32h, serum-starved for 16h, and fixed. Shown are immunofluorescence images obtained with the indicated antibodies. The merged images (c, f and i) were obtained through ImageJ Stack RGB Merge plugin and indicate co-localization (yellow) of EGFR (green) and DEP-1 (red). Arrows demarcate co-localization at cell borders and junctions. One representative experiments is shown (n=3). Scale bar: 10 μm.

(B) A431 cells were incubated for 2hrs at 4°C with a radio-labeled EGF (20 ng/ml), then washed and subjected to covalent cross-linking with BS^3 (1mM). The cross-linking reaction was subsequently quenched. Cell lysates were mixed, in the absence or presence of sodium orthovanadate (0.2mM), with glutathione beads bound to purified GST, GST-DEP-1 (WT), the DA or CS mutants, and incubated for 12h at 4°C. After extensive washing, the samples were resolved by gel electrophoresis and autoradiography (top panel). Staining with Ponceau Red (bottom panel) was used to verify equal gel loading.

(C) HeLa cells were transfected with vectors encoding HA-tagged WT DEP-1, or with the CS or DA mutants. Thereafter, cells were incubated for 32h, serum-starved for 16h, and then pre-incubated (as indicated) for 30 min with a selective EGFR kinase inhibitor (AG1478; 10 μg/ml). This was followed by EGF stimulation (20ng/ml; 10 min). DEP-1 was immunoprecipitated (IP) from whole cell lysates using anti-HA-agarose beads, followed by immunoblotting (IB) with the indicated antibodies.
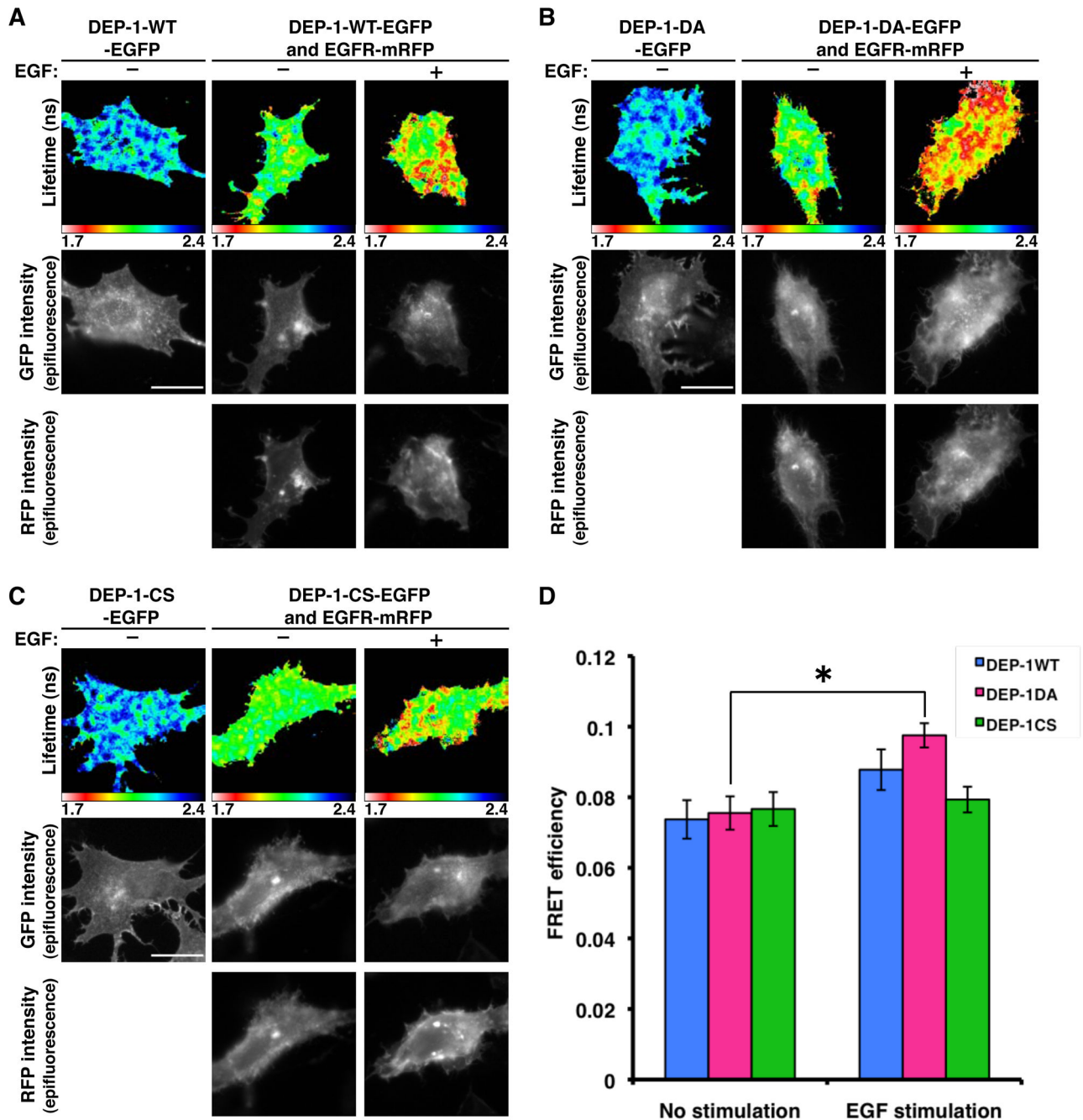
Figure 5. FRET Measurements Between DEP-1-EGFP and EGFR-mRFP Shows Specific Interactions

(A-C) MCF-7 cells were transfected with vectors encoding EGFR-mRFP, along with GFP-tagged WT DEP-1 (A), the DA mutant (B) or the CS mutant (C). Thereafter, cells were incubated for 32h, serum-starved for 16h, and stimulated with EGF (20ng/ml; 10 min), prior to fixation and fluorescence measurements. Bar: 20 μm.

(D) The mean FRET efficiency between DEP-1-EGFP and EGFR-mRFP was calculated using the following equation in each pixel and averaged per each cell. FRET efficiency = $1 - \tau da/\tau control$, where τda is the lifetime displayed by cells co-expressing both DEP-1-EGFP and EGFR-mRFP and control is the mean DEP-1-EGFP lifetime measured in the absence of

acceptor. Data are means ± SEM of 16–23 cells from three independent experiments. An asterisk refers to the DA mutant and indicates $p < 0.05$.
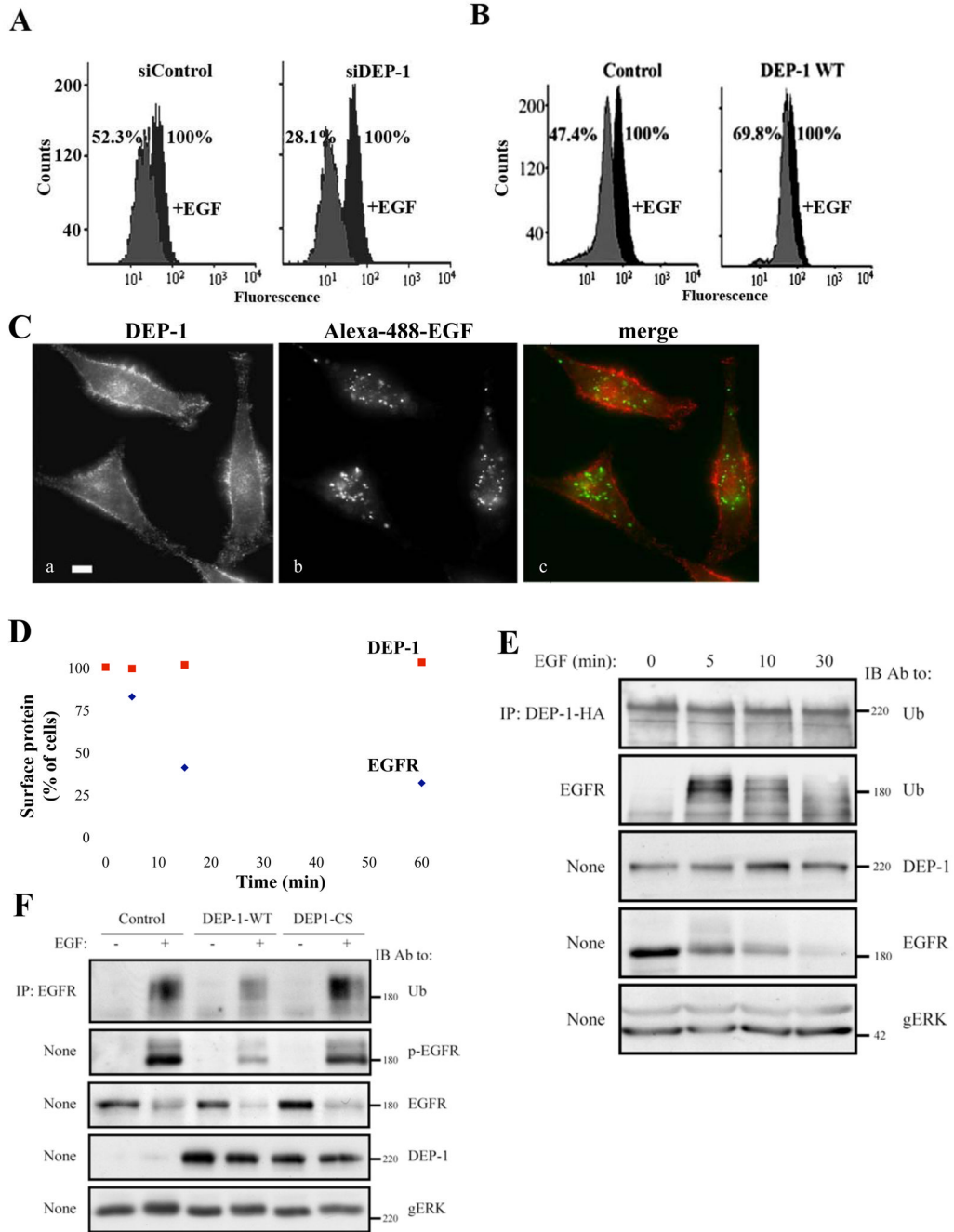
Figure 6. DEP-1 Inhibits EGFR Internalization and Ubiquitinylation and Remains on the Cell Surface After EGFR is Internalized

(A) HeLa cells were transfected with the indicated siRNA oligonucleotides, and 32h later they were starved for 16h and un-treated or treated with EGF (20ng/ml; 10 min). Thereafter, surface localized EGFR was quantified by flow cytometry. Numbers represent percents of initial cell surface EGFR.

(B) HeLa cells transiently expressing HA-DEP-1 (or a control vector) were assayed as in A. One representative experiment (n=2) is shown.

(C) HeLa cells were stimulated with a fluorescently labeled EGF (FITC-EGF; 20ng/ml) for 30 min at 22°C, fixed and analyzed by immunofluorescence using an antibody to DEP-1.

(D) HeLa cells were serum-starved for 16h and stimulated with EGF (20ng/ml) for the indicated time intervals. Thereafter, cells were surface labeled with antibodies to EGFR and DEP-1. The remaining surface fraction of each protein was quantified by flow cytometry.

(E) HeLa cells expressing DEP-1-HA were stimulated with EGF (20ng/ml) for the indicated time intervals. EGFR and the ectopically expressed DEP-1 were immunoprecipitated from cell lysates and subjected to immunoblotting.

(F) HeLa cells were treated as in E and stimulated with EGF (20ng/ml; 5 min). EGFR was analyzed by immunoblotting, either directly of after immunoprecipitation. EGFR phosphorylation was detected using an anti-phosphotyrosine antibody.
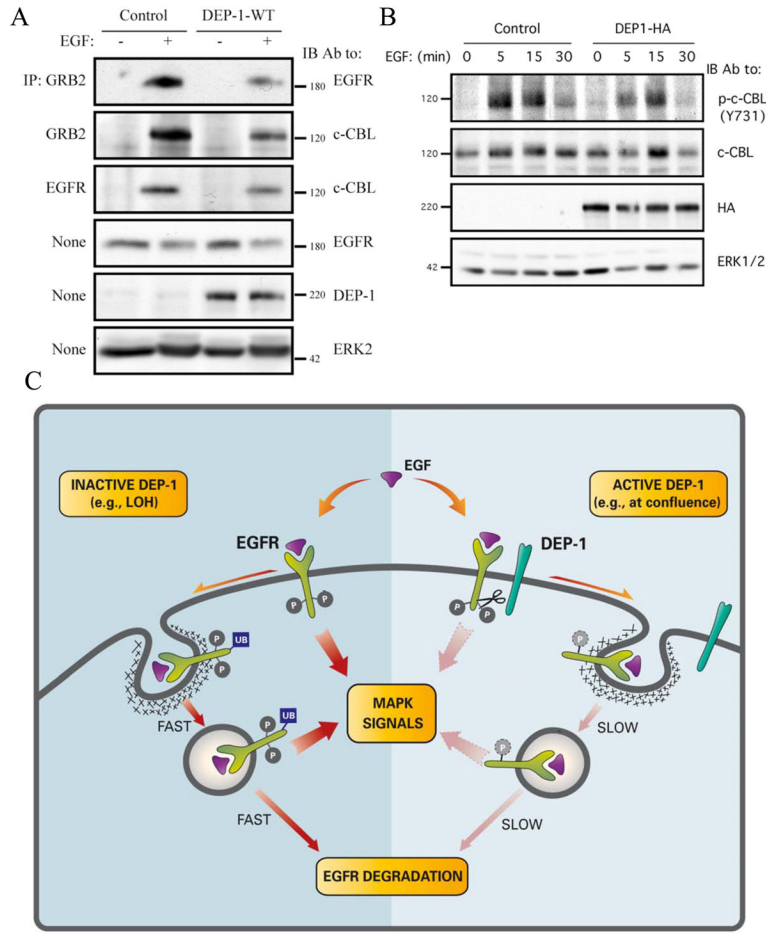
Figure 7. DEP-1 Disrupts Physical Association of an Ubiquitin Ligase Complex with EGFR Molecules and Impairs Its Activation

(A and B) HeLa cells were transfected with control or DEP-1-HA plasmids, incubated for 32h, serum-starved for 16h and stimulated with EGF (20ng/ml) for either 5min (A) or for the indicated time intervals. Whole cell lysates were immunoblotted with the indicated antibodies. (C) A model presenting the effect of DEP-1 on EGFR signalling and endocytosis: a complex comprising EGFR and DEP-1 pre-exists at the surface, especially in highly confluent epithelia. On EGF binding and receptor phosphorylation (*P*), DEP-1 dephosphorylates EGFR, thereby inhibits receptor ubiquitinylation (*Ub*) by c-CBL, which decelerates the rate of receptor internalization and diminishes MAPK signals generated at the membrane and in endosomes. When DEP-1 is inactive, for example due to loss of heterozygosity (LOH), EGFR is hyperphosphorylated and accordingly it relays strong signals to MAPK, although it gains fast rates of internalization and degradation.